Chapter III
A natural neighbours method for linear elastic problems based on Fraeijs de Veubeke variational principle

Content

Summary

In this chapter, linear elastic problems in 2D are treated with a new approach of the natural neighbours method (NEM) based on the FRAEIJS de VEUBEKE (FdV) variational principle.

In the spirit of the NEM, the domain is decomposed into N Voronoi cells corresponding to the N nodes distributed inside the domain and on its boundary.

The following discretization hypotheses are admitted:

1. The assumed displacements are interpolated between the nodes with the Laplace interpolation function.

2. The assumed support reactions are constant over each edge K of Voronoi cells on which displacements are imposed.

3. The assumed stresses are constant over each Voronoi cell.

4. The assumed strains are constant over each Voronoi cell.

Introducing these hypotheses in the FdV variational principle produces the set of equations governing the discretized solid.

These equations do not require the calculation of the derivatives of the Laplace interpolation functions and, in the absence of body forces, they only involve numerical integrations on the edges of the Voronoi cells.

These equations are recast in matrix form and it is shown that the discretization parameters associated with the assumptions on the stresses and on the strains can be eliminated at the Voronoi cell level so that the final system of equations only involves the nodal displacements and the assumed support reactions.

These support reactions can be further eliminated from the equation system if the imposed support conditions only involve displacements imposed as constant (in particular displacements imposed to zero) on a part of the solid contour.

Several applications are used to evaluate the method.

A set of patch tests are performed and show that this approach can pass the patch test up to machine precision and that there is no incompressibility locking.

Convergence studies are also made for the case of pure bending of a beam and the numerical solution is compared to the analytical solution of the Theory of Elasticity.

Finally, the case of a square membrane with a hole is also used for convergence evaluation and for comparison with the finite elements solution.
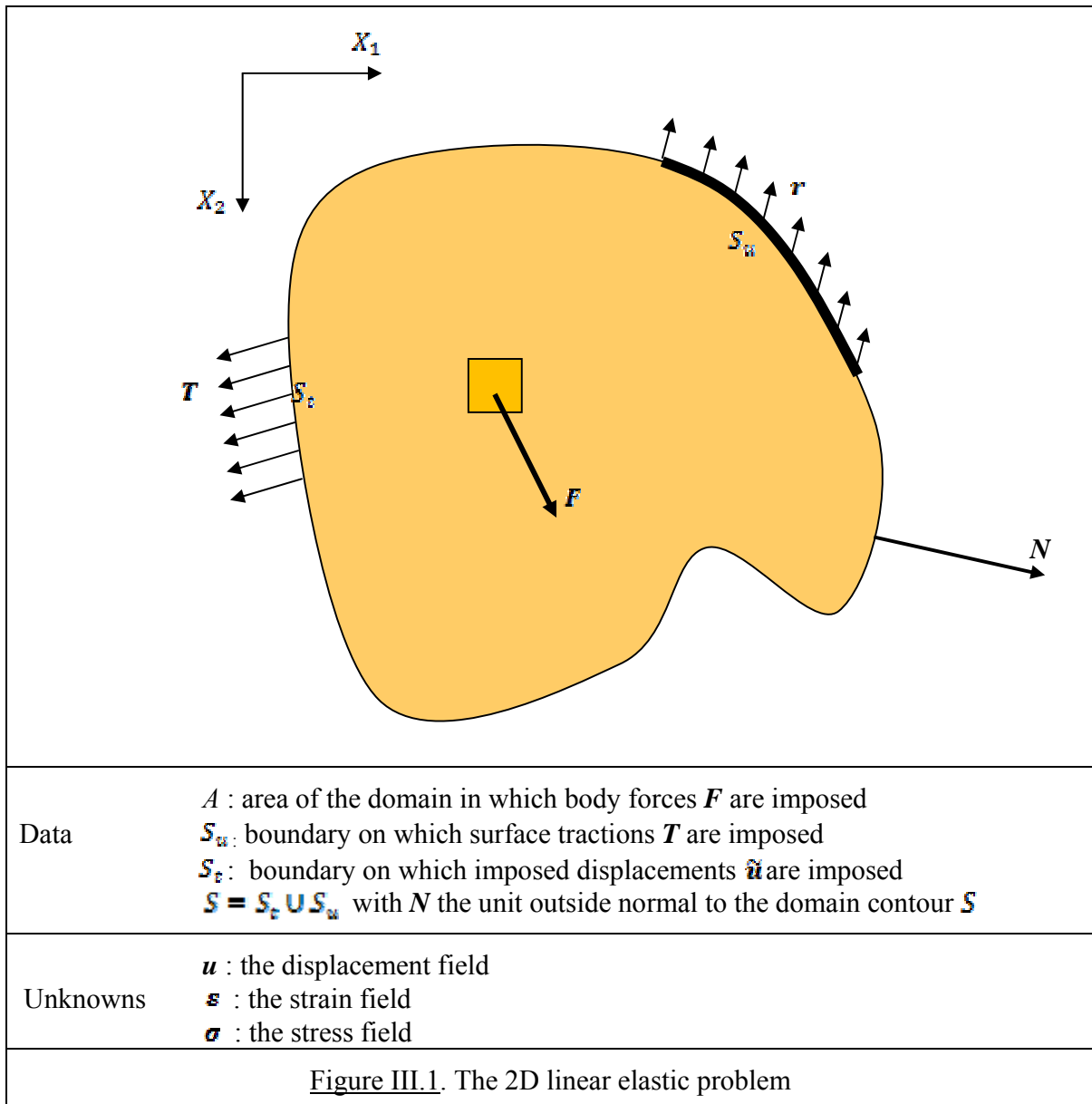
With the present approach, in the absence of body forces, the calculation of integrals over the area of the domain is avoided: only integrations on the edges of the Voronoi cells are required, for which classical Gauss numerical integration with 2 integration points is sufficient to pass the patch test. In addition, the derivatives of the nodal shape functions are not required in the resulting formulation.

The present method also allows solving problems involving nearly incompressible materials without locking.

III.1. Introduction

The present chapter develops a new numerical approach for the solution of 2D linear elastic problems.

The data and unknowns are summarized in figure III.1.

Data	A : area of the domain in which body forces F are imposed S_u : boundary on which surface tractions T are imposed S_t : boundary on which imposed displacements $\tilde{u}$ are imposed $S = S_t \cup S_u$ with N the unit outside normal to the domain contour S
Unknowns	u : the displacement field ε : the strain field σ : the stress field
Figure III.1. The 2D linear elastic problem	

In chapter II, section II.2, the classical approach of the natural neighbours method has been introduced.

The domain contains N nodes (including nodes on the contour) and the N Voronoi cells corresponding to these nodes are built.

We have seen that:

- the enforcement of boundary conditions of the type $u_i = \tilde{u}_i$ on S_u poses no difficulty if the displacements are interpolated by the Laplace interpolation functions;

- the numerical evaluation of the integrals over the area A of the domain (or, equivalently on the area of the Voronoi cells) deserves special attention;

- the "stabilized conforming nodal integration" provides an efficient solution for avoiding numerical integration on the Voronoi cells and replaces it by an integral on their contours.

In the present chapter, we will start from the FRAEIJS de VEUBEKE (FdV) variational principle (chapter II, section II.3) to develop a new approach of the natural neighbours method (NEM).

With this approach, we will see that:

- the derivatives of the Laplace interpolation functions are not necessary

- only numerical integration on the edges of the Voronoi cells are required

- incompressibility locking is avoided

III.2. Domain decomposition

Since we use the NEM, the domain is decomposed into the N Voronoi cells corresponding to the N nodes of the domain, including the nodes on the contour.

The area of the domain is:

$$A = \sum_{I=1}^{N} A_I \tag{III.1}$$

with A_I the area of Voronoi cell I.

We denote C_I the contour of Voronoi cell I.

The domain contour is the union of some of the edges of the exterior Voronoi cells. These edges are denoted by S_K and we have

$$S = \sum_{K=1}^{M} S_K \; ; \qquad S_u = \sum_{K=1}^{M_u} S_K \; ; \quad S_t = \sum_{K=1}^{M_t} S_K \; ; \qquad S = S_u \cup S_t \Rightarrow M = M_u + M_t \tag{III.2}$$

where M is the number of edges composing the contour, M_u the number of edges on which displacements $\tilde{u}_i$ are imposed and M_t the number of edges on which surface tractions T_i are imposed.

We start from the FdV variational principle introduced in chapter II and we recall its expression for completeness (we keep the equation numbers of chapter II).

$$\delta\Pi = \int_A (\sigma_{ij} - \Sigma_{ij})\delta\varepsilon_{ij}dA - \int_A (\frac{\partial \Sigma_{ji}}{\partial X_j} + F_i)\delta u_i\, dA + \int_A \delta\Sigma_{ij}\left[\frac{1}{2}(\frac{\partial u_i}{\partial X_j} + \frac{\partial u_j}{\partial X_i}) - \varepsilon_{ij}\right]dA$$

$$+ \int_{S_u}(N_j\Sigma_{ji} - r_i)\delta u_i\, dS + \int_{S_t}(N_j\Sigma_{ji} - T_i)\delta u_i\, dS + \int_{S_u}\delta r_i(\tilde{u}_i - u_i)\, dS = 0 \qquad (\text{II.36})$$

or

$$\delta\Pi = \delta\Pi_1 + \delta\Pi_2 + \delta\Pi_3 + \delta\Pi_4 + \delta\Pi_5 + \delta\Pi_6 = 0 \qquad (\text{II.31})$$

with the different terms

$$\delta\Pi_1 = \int_A \delta W(\varepsilon_{ij})dA = \int_A \sigma_{ij}\delta\varepsilon_{ij}dA \qquad (\text{II.25})$$

$$\delta\Pi_2 = \int_A \Sigma_{ij}\left[\frac{1}{2}(\frac{\partial \delta u_i}{\partial X_j} + \frac{\partial \delta u_j}{\partial X_i}) - \delta\varepsilon_{ij}\right]dA \qquad (\text{II.26})$$

$$\delta\Pi_3 = \int_A \delta\Sigma_{ij}\left[\frac{1}{2}(\frac{\partial u_i}{\partial X_j} + \frac{\partial u_j}{\partial X_i}) - \varepsilon_{ij}\right]dA \qquad (\text{II.27})$$

$$\delta\Pi_4 = -\int_A F_i\,\delta u_i\, dA \qquad (\text{II.28})$$

$$\delta\Pi_5 = -\int_{S_t} T_i\,\delta u_i\, dS \qquad (\text{II.29})$$

$$\delta\Pi_6 = \int_{S_u}\delta r_i(\tilde{u}_i - u_i)\, dS - \int_{S_u} r_i\,\delta u_i\, dS \qquad (\text{II.30})$$

For the linear elastic case, the stresses are given by:

$$\sigma_{ij} = \frac{\partial W(\varepsilon_{ij})}{\partial \varepsilon_{ij}} \qquad (\text{II.34})$$

and

$$W(\varepsilon_{ij}) = \frac{1}{2}C_{ijkl}\,\varepsilon_{ij}\,\varepsilon_{kl} \qquad (\text{II.35})$$

where C_{ijkl} is the classical Hooke's tensor.

Using the above domain decomposition, these terms become:

$$\delta\Pi_1 = \sum_{I=1}^{N}\int_{A_I}\sigma_{ij}\delta\varepsilon_{ij}\,dA_I \qquad (\text{III. 3})$$

$$\delta\Pi_2 = \sum_{I=1}^{N}\int_{A_I}\Sigma_{ij}\left[\frac{1}{2}(\frac{\partial \delta u_i}{\partial X_j} + \frac{\partial \delta u_j}{\partial X_i}) - \delta\varepsilon_{ij}\right]dA_I \qquad (\text{III. 4})$$

$$\delta \Pi_3 = \sum_{I=1}^{N} \int_{A_I} \delta \Sigma_{ij} \left[\frac{1}{2} (\frac{\partial u_i}{\partial X_j} + \frac{\partial u_j}{\partial X_i}) - \varepsilon_{ij} \right] dA_I \tag{III. 5}$$

$$\delta \Pi_4 = -\sum_{I=1}^{N} \int_{A_I} F_i \, \delta u_i \, dA_I \tag{III. 6}$$

$$\delta \Pi_5 = -\sum_{K=1}^{M_t} \int_{S_K} T_i \, \delta u_i \, dS_K \tag{III. 7}$$

$$\delta \Pi_6 = \sum_{K=1}^{M_u} \left[\int_{S_K} \delta r_i \, (\tilde{u}_i - u_i) \, dS_K - \int_{S_K} r_i \, \delta u_i \, dS_K \right] \tag{III. 8}$$

III.3. Discretization

We make the following discretization hypotheses:

1. The assumed strains ε_{ij} are constant over each Voronoi cell I:

    $$\varepsilon_{ij} = \varepsilon_{ij}^I \tag{III. 9}$$

2. The asumed stresses Σ_{ij} are constant over each Voronoi cell I:

    $$\Sigma_{ij} = \Sigma_{ij}^I \tag{III.10}$$

3. The assumed support reactions r_i are constant over each edge K of Voronoi cells on which displacements are imposed:

    $$r_i = r_i^K \tag{III. 11}$$

4. The assumed displacements u_i are interpolated by Laplace interpolation functions:

    $$u_i = \sum_{J=1}^{N} \Phi_J u_i^J \tag{III. 12}$$

    where u_i^J is the displacement of node J (corresponding to the Voronoi cell J).

Some details on the Laplace interpolation functions were given in chapter II, section II.1.2.

As a consequence of (II.34) and (III. 9), the stresses σ_{ij} are constant over each Voronoi cell I:

$$\sigma_{ij} = \sigma_{ij}^I \tag{III. 13}$$

The variations of the independent variables are:

$$\delta \varepsilon_{ij} = \delta \varepsilon_{ij}^I \tag{III. 14}$$

$$\delta\Sigma_{ij} = \delta\Sigma_{ij}^I \tag{III. 15}$$

$$\delta r_i = \delta r_i^K \tag{III. 16}$$

$$\delta u_i = \sum_{I=1}^N \Phi_I \delta u_i^I \tag{III. 17}$$

Introducing these assumptions in (III. 3) to (III. 5), and integrating by parts, we get:

$$\delta\Pi_1 = \sum_{I=1}^N \sigma_{ij}^I \delta\varepsilon_{ij}^I A_I \tag{III. 18}$$

$$\delta\Pi_2 = \sum_{I=1}^N \Sigma_{ij}^I \int_{A_I} \left[\frac{1}{2}(\frac{\partial\delta u_i}{\partial X_j} + \frac{\partial\delta u_j}{\partial X_i}) \right] dA_I - \sum_{I=1}^N \Sigma_{ij}^I \delta\varepsilon_{ij}^I A_I =$$

$$\sum_{I=1}^N \Sigma_{ij}^I \oint_{C_I} N_j^I \delta u_i \, dC_I - \sum_{I=1}^N \Sigma_{ij}^I \delta\varepsilon_{ij}^I A_I \tag{III. 19}$$

$$\delta\Pi_3 = \sum_{I=1}^N \delta\Sigma_{ij}^I \int_{A_I} \left[\frac{1}{2}(\frac{\partial u_i}{\partial X_j} + \frac{\partial u_j}{\partial X_i}) \right] dA_I - \sum_{I=1}^N \delta\Sigma_{ij}^I \varepsilon_{ij}^I A_I =$$

$$\sum_{I=1}^N \delta\Sigma_{ij}^I \oint_{C_I} N_j^I u_i \, dC_I - \sum_{I=1}^N \delta\Sigma_{ij}^I \varepsilon_{ij}^I A_I \tag{III. 20}$$

$$\delta\Pi_6 = \sum_{K=1}^{M_u} \left[\delta r_i^K \int_{S_K} (\widetilde{u}_i - u_i) dS_K - r_i^K \int_{S_K} \delta u_i dS_K \right] \tag{III. 21}$$

where N_j^I is the unit outward normal to the contour of Voronoi cell *I*.

Introducing in (II.31), we get:

$$\delta\Pi = \delta\Pi_{VA} + \delta\Pi_{VC} + \delta\Pi_{DC} + \delta\Pi_{EF} = 0 \tag{III. 22}$$

with

$$\delta\Pi_{VA} = \sum_{I=1}^N (\sigma_{ij}^I - \Sigma_{ij}^I)\delta\varepsilon_{ij}^I A_I - \sum_{I=1}^N \delta\Sigma_{ij}^I \varepsilon_{ij}^I A_I \tag{III. 23}$$

$$\delta\Pi_{VC} = \sum_{I=1}^N \Sigma_{ij}^I \oint_{C_I} N_j^I \delta u_i \, dC_I + \sum_{I=1}^N \delta\Sigma_{ij}^I \oint_{C_I} N_j^I u \, dC_I \tag{III. 24}$$

$$\delta\Pi_{DC} = \sum_{K=1}^{M_u} \left[\delta r_i^K \int_{S_K} (\widetilde{u}_i - u_i) dS_K - r_i^K \int_{S_K} \delta u_i dS_K \right] \tag{III. 25}$$

$$\delta\Pi_{EF} = -\sum_{I=1}^{N}\int_{A_I} F_i\,\delta u_i\,dA_I - \sum_{K=1}^{M_t}\int_{S_K} T_i^K\,\delta u_i\,dS_K \qquad\qquad \text{(III. 26)}$$

In (III. 24) to (III. 26), the displacements and virtual displacements are interpolated by (III. 12) and (III. 17) respectively. Substituting in (III. 24), we get:

$$\delta\Pi_{VC} = \sum_{I=1}^{N}\Sigma_{ij}^{I}\left[\sum_{J=1}^{N}\oint_{C_I} N_j^I\Phi_J\delta u_i^J\,dC_I\right] + \sum_{I=1}^{N}\delta\Sigma_{ij}^{I}\left[\sum_{J=1}^{N}\oint_{C_I} N_j^I\Phi_J u_i^J\,dC_I\right] \qquad\qquad \text{(III. 27)}$$

Finally, since the edges of Voronoi cell are straight lines, the outer normal N_j to edge S_K is constant along this edge and is denoted N_j^K

Now, using the discretization (III. 12), we get:

$$\delta\Pi_{DC} = \sum_{K=1}^{M_u}\delta r_i^K\left\{\int_{S_K}\widetilde{u}_i\,dS_K - \sum_{J=1}^{N} u_i^J\int_{s_K}\Phi_J\,dS_K\right\} - \sum_{K=1}^{M_u} r_i^K\left\{\sum_{J=1}^{N}\delta u_i^J\int_{S_K}\Phi_J\,dS_K\right\} \qquad\qquad \text{(III. 28)}$$

Similarly, (III. 26) becomes:

$$\delta\Pi_{EF} = -\sum_{I=1}^{N}\sum_{J=1}^{N}\delta u_i^J\int_{A_I} F_i\,\Phi_J\,dA_I - \sum_{K=1}^{M_t}\sum_{J=1}^{N}\delta u_i^J\int_{S_K} T_i\,\Phi_J\,dS_K \qquad\qquad \text{(III. 29)}$$

Collecting all the results, we obtain the discretized FdV variational principle.

$$\delta\Pi = \sum_{I=1}^{N}(\sigma_{ij}^I - \Sigma_{ij}^I)\delta\varepsilon_{ij}^I A_I - \sum_{I=1}^{N}\delta\Sigma_{ij}^I\varepsilon_{ij}^I A_I$$

$$+ \sum_{I=1}^{N}\Sigma_{ij}^I\left\{\sum_{J=1}^{N}\delta u_i^J\oint_{C_I} N_j^I\Phi_J\,dC_I\right\}$$

$$+ \sum_{I=1}^{N}\delta\Sigma_{ij}^I\left\{\sum_{J=1}^{N} u_i^J\oint_{C_I} N_j^I\Phi_J\,dC_I\right\}$$

$$+ \sum_{K=1}^{M_u}\delta t_i^K\left\{\int_{S_K}\widetilde{u}_i\,dS_K - \sum_{J=1}^{N} u_i^J\int_{S_K}\Phi_J\,dS_K\right\}$$

$$-\sum_{K=1}^{M_u} t_i^K \left\{ \sum_{J=1}^{N} \delta u_i^J \int_{S_K} \Phi_J dS_K \right\}$$

$$-\sum_{I=1}^{N} \sum_{J=1}^{N} \delta u_i^J \int_{A_I} F_i \Phi_J \, dA_I - \sum_{K=1}^{M_t} \sum_{J=1}^{N} \delta u_i^J \int_{S_K} T_i \Phi_J \, dS_K \quad = 0 \qquad \text{(III. 30)}$$

III.4. Equations deduced from the FdV variational principle

Let us reorganize the terms of (III. 30)

$$\delta\Pi = \sum_{I=1}^{N} \delta\varepsilon_{ij}^I \left\{ (\sigma_{ij}^I - \Sigma_{ij}^I) \, A_I \right\}$$

$$+ \sum_{I=1}^{N} \delta\Sigma_{ij}^I \left\{ - \varepsilon_{ij}^I \, A_I + \sum_{J=1}^{N} u_i^J A_j^{IJ} \right\}$$

$$+ \sum_{K=1}^{M_u} \delta t_i^K \left\{ \widetilde{U}_i^K - \sum_{J=1}^{N} u_i^J B^{KJ} \right\}$$

$$+ \sum_{J=1}^{N} \delta u_i^J \left\{ \sum_{I=1}^{N} (\Sigma_{ij}^I A_j^{IJ} - \widetilde{F}_i^{IJ}) - \sum_{K=1}^{M_t} \widetilde{T}_i^{KJ} \right\}$$

$$- \sum_{J=1}^{N} \delta u_i^J \left\{ \sum_{K=1}^{M_u} r_i^K B^{KJ} \right\} = 0 \qquad \text{(III.31)}$$

In this result, the following notations have been used.

$$A_j^{IJ} = \oint_{C_I} N_j^I \Phi_J \, dC_I \qquad \text{(III.32)}$$

$$B^{KJ} = \int_{S_K} \Phi_J dS_K \qquad \text{(III.33)}$$

$$\widetilde{U}_i^K = \int_{S_K} \widetilde{u}_i dS_K \qquad \text{(III.34)}$$

$$\widetilde{F}_i^{IJ} = \int_{A_I} F_i \Phi_J \, dA_I \qquad \text{(III.35)}$$

$$\widetilde{T}_i^{KJ} = \int_{S_K} T_i \Phi_J \, dS_K \qquad \text{(III.36)}$$

Equation (III.32) involves the integration on the contour C_I of Voronoi cell I.

Equations (III.33) and (III.34) involve the integration on the edge S_K (belonging to the domain contour) of an exterior Voronoi cell.

We are now able to deduce the Euler equations.

1. In all the Voronoi cells I

$$\sigma_{ij}^I = \Sigma_{ij}^I \qquad \text{for} \quad I = 1, N \tag{III.37}$$

These equations identify the assumed stresses Σ_{ij}^I as the constitutive stresses σ_{ij}^I deduced from the assumed strains ε_{ij}^I in each Voronoi cell.

2. In all the Voronoi cells I

$$\varepsilon_{ij}^I A_I = \sum_{J=1}^N u_i^J A_j^{IJ} \quad \text{for} \quad I = 1, N \tag{III.38}$$

This is a compatibility equation linking the assumed strains ε_{ij}^I in Voronoi cell I with the assumed nodal displacements u_i^J.

3. On the edges K of Voronoi cells submitted to imposed displacements

$$\sum_{J=1}^N u_i^J B^{KJ} = \widetilde{U}_i^K \qquad \text{for} \ K = 1, M_u \tag{III.39}$$

These are also compatibility equations taking account of the imposed displacements $\widetilde{u}_i$ along the domain contour.

4. In all the Voronoi cells J

$$\sum_{I=1}^N (\Sigma_{ij}^I A_j^{IJ} - \widetilde{F}_i^{IJ}) - \sum_{K=1}^{M_t} \widetilde{T}_i^{KJ} - \sum_{K=1}^{M_u} r_i^K B^{KJ} = 0 \quad \text{for} \quad J = 1, N \tag{III.40}$$

These are equilibrium equations taking account of the body forces F_i, the surface tractions T_i and the assumed support reactions r_i^K.

We note that, in the developments above, the only term that implies an integration over the area of the Voronoi cells is $\widetilde{F}_i^{IJ} = \int_{A_I} F_i \Phi_J \, dA_I$.

Hence, if there are no body forces, the problem of choosing integration points is simplified: there are only integrations along the straight edges of Voronoi cells. A classical Gauss integration scheme can be used. Some tests (see section III.6 below) show that 2 integration points give enough precision.

This property of the present approach eliminates the need for special integration schemes [ATLURI S.N. et al. (1999), ATLURI S.N. and ZHU T. (2000), CUETO E. et al. (2003)] over the area of the domain.

Furthermore, this formulation does not require the derivatives of the shape functions.

So, using the FdV functional as starting point, we obtain the same advantages as with the stabilized conforming nodal integration [CHEN J. S. et al. (2001), YOO J. et al. (2004)].

We also remark that, from the definition of

$$A_j^{IJ} = \oint_{C_I} N_j^I \Phi_J dC_I$$

we have

$$A_j^{IJ} = \oint_{C_I} N_j^I \Phi_J dC_I = \sum_{all\ K(I)} N_j^{K(I)} \int_{S_{K(I)}} \Phi_K dS_K$$

where $\sum\limits_{all\ K(I)}$ means the sum over all the edges $K(I)$ of the Voronoi cell I and $N_j^{K(I)}$ is the outward unit normal to that edge.

From this, we see that the calculation of the coefficients A_j^{IJ} and B^{KJ} only implies the calculation of integrals of the type $\int_{S_K} \Phi_J dS_K$ along edges of Voronoi cells.

Finally, in the approach developed here, it is possible to impose displacements $\widetilde{u}_i$ on any edge of any Voronoi cell. From (III.34) and (III.39), it is clear that the imposed displacements are respected in a weighted average sense.

III.5. Matrix notation

We introduce the following matrix notation.

$$\{\varepsilon\}^I = \begin{Bmatrix} \varepsilon_{11}^I \\ \varepsilon_{22}^I \\ 2\varepsilon_{12}^I \end{Bmatrix}; \quad \{\sigma\}^I = \begin{Bmatrix} \sigma_{11}^I \\ \sigma_{22}^I \\ \sigma_{12}^I \end{Bmatrix}; \quad \{\Sigma\}^I = \begin{Bmatrix} \Sigma_{11}^I \\ \Sigma_{22}^I \\ \Sigma_{12}^I \end{Bmatrix}; \quad \{u\}^I = \begin{Bmatrix} u_1^I \\ u_2^I \end{Bmatrix} \tag{III.41}$$

$$\{\widetilde{F}\}^{IJ} = \begin{Bmatrix} \widetilde{F}_1^{IJ} \\ \widetilde{F}_2^{IJ} \end{Bmatrix}; \quad \{\widetilde{T}\}^{KJ} = \begin{Bmatrix} \widetilde{T}_1^{KJ} \\ \widetilde{T}_2^{KJ} \end{Bmatrix}; \quad \{\widetilde{F}\}^J = \sum_{I=1}^N \{\widetilde{F}\}^{IJ}; \quad \{\widetilde{T}\}^J = \sum_{K=1}^{M_I} \{\widetilde{T}\}^{KJ} \tag{III.42}$$

$$[A]^{IJ} = \begin{bmatrix} A_1^{IJ} & 0 & A_2^{IJ} \\ 0 & A_2^{IJ} & A_1^{IJ} \end{bmatrix}; \quad \{r\}^K = \begin{Bmatrix} r_1^K \\ r_2^K \end{Bmatrix}; \quad \{\widetilde{U}\}^K = \begin{Bmatrix} \widetilde{U}_1^K \\ \widetilde{U}_2^K \end{Bmatrix} \tag{III.43}$$

Then, we get successively:

$$\sigma_{ij}^I = \Sigma_{ij}^I \Rightarrow \{\sigma\}^I = \{\Sigma\}^I \tag{III.44}$$

$$\Sigma_{ij}^I A_j^{IJ} \Rightarrow [A]^{IJ} \{\Sigma\}^I \; ; \quad \widetilde{F}^{IJ} \Rightarrow \{\widetilde{F}\}^{IJ} \; ; \quad \widetilde{T}^{IJ} \Rightarrow \{\widetilde{T}\}^{IJ} \tag{III.45}$$

$$\sum_{I=1}^N \Sigma_{ij}^I A_j^{IJ} - \sum_{K=1}^{M_u} t_i^K B^{KJ} = \sum_{I=1}^N \widetilde{F}_i^{IJ} + \sum_{K=1}^{M_t} \widetilde{T}_i^{KJ}$$

$$\Rightarrow \sum_{I=1}^N [A]^{IJ} \{\Sigma\}^I - \sum_{K=1}^{M_u} B^{KJ} \{r\}^K = \{\widetilde{F}\}^J + \{\widetilde{T}\}^J \tag{III.46}$$

The term $\sum_{I=1}^N [A]^{IJ} \{\Sigma\}^I - \sum_{K=1}^{M_u} B^{KJ} \{r\}^K$ is the interior nodal force at node J, i.e. in cell J. It is the sum of the contributions $[A]^{IJ} \{\Sigma\}^I$ of the stresses that are present in all the Voronoi cells I and of the contributions $B^{KJ} \{r\}^K$ of the support reactions r_i^K existing on the contour edges K where displacements are imposed.

The term $\{\widetilde{F}\}^J + \{\widetilde{T}\}^J$ is the exterior nodal force at node J, i.e. in cell J. It is the sum of :

- the contributions $\{\widetilde{F}\}^{IJ}$ of the body forces F_i existing in all the Voronoi cells I

- the contributions $\{\widetilde{T}\}^{IJ}$ of the surface tractions T_i applied on the part S_t of the domain contour.

Now, consider equation (III.38), it can be written

$$A_I \{\varepsilon\}^I = \sum_{J=1}^N [A]^{IJ,T} \{u\}^J \tag{III.47}$$

where $[A]^{IJ,T}$ is the transpose of $[A]^{IJ}$.

Note that in $\{\varepsilon\}^I$, the third component is $2\varepsilon_{12}^I$.

The compatibility equation (III.47) defines the strain $\{\varepsilon\}^I$ in a Voronoi cell I as the sum of the contributions $[A]^{IJ,T} \{u\}^J$ of all the nodes J.

On the edges K submitted to imposed displacements, we must consider (III.39) that becomes

$$\sum_{J=1}^N B^{KJ} \{u\}^J = \{\widetilde{U}\}^K \tag{III.48}$$

The tables III. 1 and III. 2 below collect all the results in matrix form.

In these tables, taking account of (III.37), $\{\Sigma\}^I$ is replaced by $\{\sigma\}^I$.

Table III. 1. Matrix notations for the linear elastic case	
Notations and symbols	Comments
$\{\varepsilon\}^I = \begin{Bmatrix} \varepsilon_{11}^I \\ \varepsilon_{22}^I \\ 2\varepsilon_{12}^I \end{Bmatrix}$	Strains in cell I
$\{\sigma\}^I = \begin{Bmatrix} \sigma_{11}^I \\ \sigma_{22}^I \\ \sigma_{12}^I \end{Bmatrix}$	Stresses in cell I
$\{u\}^I = \begin{Bmatrix} u_1^I \\ u_2^I \end{Bmatrix}$	Displacements of node I belonging to cell I
$\{r\}^K = \begin{Bmatrix} r_1^K \\ r_2^K \end{Bmatrix}$	Support reactions on edge K submitted to imposed displacements
$A_I \ ; \ C_I$	Area and contour of cell I
S_K	Length of edge K of a cell
Φ_J	Interpolant associated with node J
$\widetilde{F}_i^{IJ} = \int_{A_I} F_i \, \Phi_J \, dA_I \ ; \ \{\widetilde{F}\}^{IJ} = \begin{Bmatrix} \widetilde{F}_1^{IJ} \\ \widetilde{F}_2^{IJ} \end{Bmatrix} ;$ $\{\widetilde{F}\}^J = \sum_{I=1}^{N} \{\widetilde{F}\}^{IJ}$	$\{\widetilde{F}\}^J$ is the nodal force at node J equivalent to the body forces F_i applied to the solid
$\widetilde{T}_i^{KJ} = \int_{S_K} T_i \, \Phi_J \, dS_K \ ; \ \{\widetilde{T}\}^{KJ} = \begin{Bmatrix} \widetilde{T}_1^{KJ} \\ \widetilde{T}_2^{KJ} \end{Bmatrix} ;$ $\{\widetilde{T}\}^J = \sum_{K=1}^{M_I} \{\widetilde{T}\}^{KJ}$	$\{\widetilde{T}\}^J$ is the nodal force at node J equivalent to the surface tractions T_i applied to the contour of the solid
$\widetilde{U}_i^K = \int_{S_K} \widetilde{u}_i \, dS_K \ ; \ \{\widetilde{U}\}^K = \begin{Bmatrix} \widetilde{U}_2^K \\ \widetilde{U}_1^K \end{Bmatrix}$	$\{\widetilde{U}\}^K$ is a generalized displacement taking account of imposed displacements $\widetilde{u}_i$ on edge K
$B^{KJ} = \int_{S_K} \Phi_J \, dS_K$	Integration over the edge K of a cell
$A_j^{IJ} = \oint_{C_I} N_j^I \Phi_J \, dC_I \ ; \ [A]^{IJ} = \begin{bmatrix} A_1^{IJ} & 0 & A_2^{IJ} \\ 0 & A_2^{IJ} & A_1^{IJ} \end{bmatrix}$	A_j^{IJ} can also be computed by $A_j^{IJ} = \sum_{all\ K(I)} N_j^{K(I)} B^{K(I)J}$

Table III. 2. Discretized equations in matrix form for the linear elastic case		
Equations	Comments	
$$\sum_{I=1}^{N}[A]^{IJ}\{\Sigma\}^{I} - \sum_{K=1}^{M_u}B^{KJ}\{r\}^{K} = \{\widetilde{F}\}^{J} + \{\widetilde{T}\}$$	Equilibrium equation of cell J	(III.49)
$$A_I\{\varepsilon\}^{I} = \sum_{J=1}^{N}[A]^{IJ,T}\{u\}^{J}$$	Compatibility equation for cells I	(III.50)
$$\sum_{J=1}^{N}B^{KJ}\{u\}^{J} = \{\widetilde{U}\}^{K}$$	Compatibility equation on edge K submitted to imposed displacements	(III.51)

If we consider a linear elastic material, the constitutive equation for a Voronoi cell J is

$$\{\sigma\}^{J} = [C]^{J}\{\varepsilon\}^{J} \tag{III.52}$$

where $[C]^{J}$ is the Hooke compliance matrix of the elastic material composing cell J. Introducing (III.50) in (III.52), we get

$$\{\sigma\}^{J} = [C]^{J}\{\varepsilon\}^{J} = [C^*]^{J}\sum_{J=1}^{N}[A]^{IJ,T}\{u\}^{J} \tag{III.53}$$

with

$$[C^*]^{J} = \frac{1}{A^{J}}[C]^{J} \tag{III.54}$$

Then

$$\sum_{I=1}^{N}[A]^{IJ}\{\Sigma\}^{I} = \sum_{L=1}^{N}(\sum_{I=1}^{N}[A]^{IJ}[C^*]^{I}[A]^{IL,T})\{u\}^{L} = \sum_{L=1}^{N}[M]^{JL}\{u\}^{L} \tag{III.55}$$

with

$$[M]^{JL} = \sum_{I=1}^{N}[A]^{IJ}[C^*]^{I}[A]^{IL,T} \tag{III.56}$$

Replacing in (III.49), we obtain:

$$\sum_{L=1}^{N}[M]^{JL}\{u\}^{L} - \sum_{K=1}^{M_u}B^{KJ}\{r\}^{K} = \{\widetilde{F}\}^{J} + \{\widetilde{T}\} \tag{III.57}$$

$$\sum_{L=1}^{N}[M]^{JL}\{u\}^{L} = \sum_{K=1}^{M_u}B^{KJ}\{r\}^{K} + \{\widetilde{F}\}^{J} + \{\widetilde{T}\} \tag{III.58}$$

$$\sum_{J=1}^{N} B^{KJ} \{u\}^{J} = \{\widetilde{U}\}^{K} \qquad (\text{III.59})$$

Equations (III.58) and (III.59) constitute an equation system of the form:

$$\begin{bmatrix} [M] & -[B] \\ -[B]^{T} & [0] \end{bmatrix} \begin{Bmatrix} \{q\} \\ \{r\} \end{Bmatrix} = \begin{Bmatrix} \{\widetilde{Q}\} \\ -\{\widetilde{U}\} \end{Bmatrix} \qquad (\text{III.60})$$

with

$$\{q\} = \begin{Bmatrix} \{u\}^{1} \\ \{u\}^{2} \\ . \\ . \\ \{u\}^{N} \end{Bmatrix}; \quad \{\widetilde{F}\} = \begin{Bmatrix} \{\widetilde{F}\}^{1} \\ \{\widetilde{F}\}^{2} \\ . \\ . \\ \{\widetilde{F}\}^{N} \end{Bmatrix}; \quad \{\widetilde{T}\} = \begin{Bmatrix} \{\widetilde{T}\}^{1} \\ \{\widetilde{T}\}^{2} \\ . \\ . \\ \{\widetilde{T}\}^{N} \end{Bmatrix}; \quad \{\widetilde{Q}\} = \{\widetilde{F}\} + \{\widetilde{T}\} \qquad (\text{III.61})$$

$$[M] = \begin{bmatrix} [M]^{11} & [M]^{12} & . & . & [M]^{1N} \\ [M]^{21} & [M]^{22} & . & . & [M]^{2N} \\ . & & . & . & . \\ . & . & . & . & . \\ [M]^{N1} & [M]^{N2} & . & . & [M]^{NN} \end{bmatrix}; \quad [B] = \begin{bmatrix} [B]^{11} & [B]^{12} & . & . & [B]^{1M_{u}} \\ [B]^{21} & [B]^{22} & . & . & [B]^{2M_{u}} \\ . & & . & . & . \\ . & . & . & . & . \\ [B]^{N1} & [B]^{N2} & . & . & [B]^{NM_{u}} \end{bmatrix} \qquad (\text{III.62})$$

It can be easily verified that matrix $[M]$ is symmetric.

Equations (III.51) that, in matrix form, become $[B]^{T}\{q\} = \{\widetilde{U}\}$ constitute a set of constraints on the nodal displacements $\{q\}$.

In particular, if displacements $\widetilde{u}_{i} = 0$ are imposed on the segment AB joining 2 nodes A and B on the domain contour, it is easy to show that (III.51) leads to $u_{i}^{A} = 0$ and $u_{i}^{B} = 0$.

In such a case, the displacements u_{i}^{A} and u_{i}^{B} can be removed from the unknowns $\{q\}$.

This reasoning can be extended to the case of displacements imposed to 0 on any number of similar segments belonging to the contour.

This shows that, despite of the fact that in the initial assumptions (III.9) to (III.12) many discretization parameters appear, most of them are eliminated at the Voronoi cell level, which finally leads to an equation system of the classical form $[M]\{q\} = \{\widetilde{Q}\}$ with the same characteristics as in the classical approach based on the virtual work principle.

III.6. Numerical integration

For the numerical integration of integrals of the type $\int_{S_K} \Phi_J dS_K$, Gauss method is used.

Using a local coordinate $-1 \leq \xi \leq +1$ along edge S_K, such an integral takes the form:

$$\int_{-1}^{1} f(\xi) d\xi = \sum_{IP=1}^{NP} f(\xi_{IP}) W(IP) \tag{III.63}$$

in which IP denotes the integration point, NP the number of integration points, ξ_{IP} the coordinate of integration point IP and $W(IP)$ the weight of integration point IP.

The precision of the scheme has been tested from one to ten integration points. To achieve this, advantage is taken from the fact that the calculation of $A_j^{IJ} = \oint_{C_I} n_j^I \phi_J dS_I$ can be performed analytically for a regular distribution of nodes on a square pattern as developed in annex 1.

Table III.3 gives the results for $A_1^{IJ} = \oint_{C_I} N_1^I \phi_J dS_I$; $A_2^{IJ} = \oint_{C_I} N_2^I \phi_J dS_I$

Table III. 3. Tests for the numerical integration along an edge of a Voronoi cell.										
Integration points	$NP=1$	$NP=2$	$NP=3$	$NP=4$	$NP=5$	$NP=6$	$NP=7$	$NP=8$	$NP=9$	$NP=10$
Relative error on A_1^{IJ} (%)	30.13	0.77	4.52	2.62	0.75	0.99	1.72	0.59	0.24	0.57
Relative error on A_2^{IJ} (%)	12.82	0.32	1.85	1.08	0.31	0.41	0.71	0.24	0.10	0.24

It is seen that the precision does not necessarily increase with the number of integration points. From table III.3, it was decided to use $NP=2$ in all the subsequent calculations.

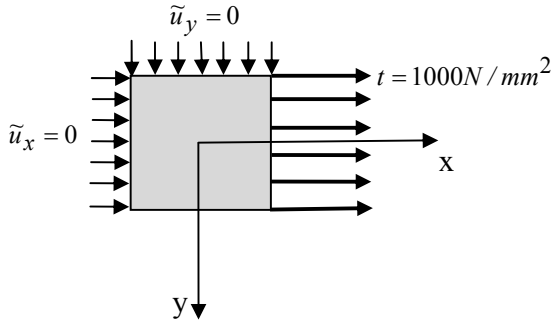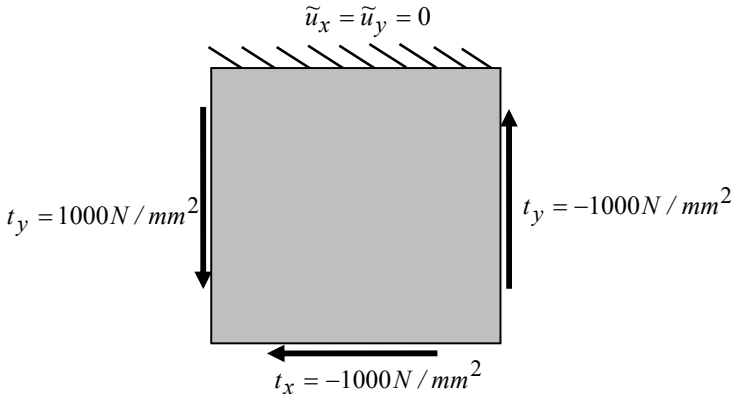## III.7. Applications

III.7.1. Patch tests

A set of patch tests in simple tension and in pure shear are performed to validate the method. Unit thickness and plane strain conditions are assumed.
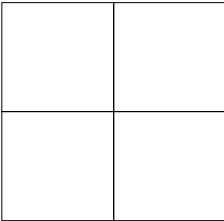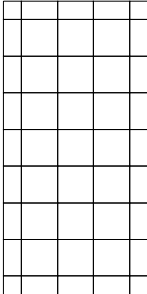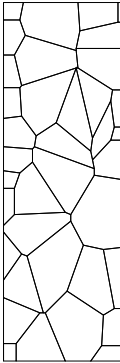
The domain, the loading, the nodes and the Voronoi cells for the 5 case studies are given in figures III.2 and III.3

The results are given in tables III.4 and table III.5 for two different Poisson's ratios: $\nu = 0.$ and $\nu = 0.3$. They are expressed with the help of the following variables.

$$Average = \frac{\sum\limits_{K=1}^{N} \sigma^K}{N} \; ; \quad L2\,norm = \frac{\sum\limits_{K=1}^{N} A_K \sqrt{(\sigma_{ij}^K - \sigma_{ij}^{exact})(\sigma_{ij}^K - \sigma_{ij}^{exact})} / \sum\limits_{K=1}^{N} A_K}{\sum\limits_{K=1}^{N} A_K \sqrt{\sigma_{ij}^{exact}\sigma_{ij}^{exact}} / \sum\limits_{K=1}^{N} A_K} \qquad \text{(III.64)}$$

Case number and configuration	Loadings and boundary conditions
Case 1: square Case 2: rectangular Case 3: rectangular	
Case4: square Case 5: rectangular	
	Figure III.2. Loadings and boundary conditions for the patch tests.

Case number and number of nodes	Voronoi cells
Case1: 4 nodes Case 4: 4 nodes	
Case2: 45 nodes	
Case3: 38 nodes Case 5: 38 nodes	
Figure III.3. Voronoi cells for the patch tests	

Table III.4. Results of the 5 patch tests with $E = 10^8\, N/mm^2$ and $\nu = 0.3$							
Case	Configu-ration	Loading	N	σ_{11} average (N/mm^2)	σ_{22} average (N/mm^2)	σ_{12} average (N/mm^2)	L2 norm
1	Square	Simple tension	4	1000	-4.42E-12	1.11E-11	2.87E-16
2	Rectangular regular cells	Simple tension	45	2.94E-13	1000	-3.67E-12	5.11E-17
3	Rectangular irregular cells	Simple tension	38	-7.44E-12	1000	2.16E-11	9.97E-16
4	Square	Pure shear	4	1.88E-12	-3.99E-17	-1000	3.77E-16
5	Rectangular irregular cells	Pure shear	38	8.85E-12	7.13E-12	-1000	7.43E-16

Table III.5. Results of the 5 patch tests with $E = 10^8\, N/mm^2$ and $\nu = 0.3$							
Case	Configu-ration	Loading	N	σ_{11} average (N/mm^2)	σ_{22} average (N/mm^2)	σ_{12} average (N/mm^2)	L2 norm
1	Square	Simple tension	4	1000	-4.42E-12	1.11E-10	2.87E-16
2	Rectangular regular cells	Simple tension	45	2.94E-12	1000	-3.67E-12	5.11E-17
3	Rectangular irregular cells	Simple tension	38	-1.44E-12	1000	5.16E-11	3.10E-16
4	Square	Pure shear	4	1.92E-12	-1.74E-13	-1000	1.77E-16
5	Rectangular irregular cells	Pure shear	38	1.37E-12	-4.64E-12	-1000	7.43E-16

These results are computed with 2 integration points on each edge of the Voronoi cells *(NP=2)*.

Results with *NP=9* were also computed but are not significantly different.

It is seen that the patch tests are satisfied up to machine precision.

For case 3, results for a nearly incompressible material with $\nu = 0.49$, $\nu = 0.499$, $\nu = 0.4999$ have also been computed. They are summarized in table III.6 that shows some decrease in the precision of the results.

Table III.6. Results of patch tests (case 3) for a nearly incompressible material	
ν	L2 norm
0.3	3.10E-16
0.49	5.14E-15
0.499	1.95E-14
0.4999	4.70E-13

In fact, this is a problem linked with the deterioration of the conditioning of matrix $[M]$ in (III.60) [WILKINSON, JH. (1965), FRIED I. (1973)].

If there is a small error $[M_e]$ on $[M]$ because of machine precision, the solution is modified and becomes $\{q\} + \{q_e\}$.

According to [WILKINSON, JH. (1965)]:

$$\frac{\|q_e\|}{\|q\|} \leq C \frac{\|M_e\|}{\|M\|} \bigg/ \left[1 - C \frac{\|M_e\|}{\|M\|} \right] \tag{III.65}$$

in which $\| \ \|$ is the L2 norm.

If $\|M_e\| << \|M\|$, this result becomes approximately:

$$\frac{\|q_e\|}{\|q\|} \leq C \frac{\|M_e\|}{\|M\|} \tag{III.66}$$

where C is the condition number of $[M]$.

For a 3D solid discretized in tetrahedral finite elements of size h, it has been shown in [FRIED (1973)] that :

$$C = c \frac{h^{-2}}{(1+v)(1-2v)} \tag{III.67}$$

where c is a constant and h is the size of the elements.

Although this result has not been established in the frame of the natural neighbours method, a simple calculation shows that, when v changes from 0.49 to 0.499 or 0.4999, the error on the solution is multiplied by 10 or 100 or 1000, which explains the results observed in table III.6.

This shows that the patch tests can be passed also for nearly incompressible materials.
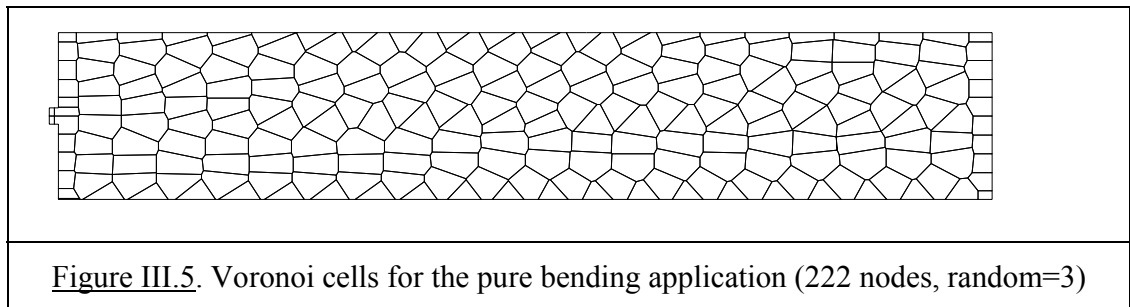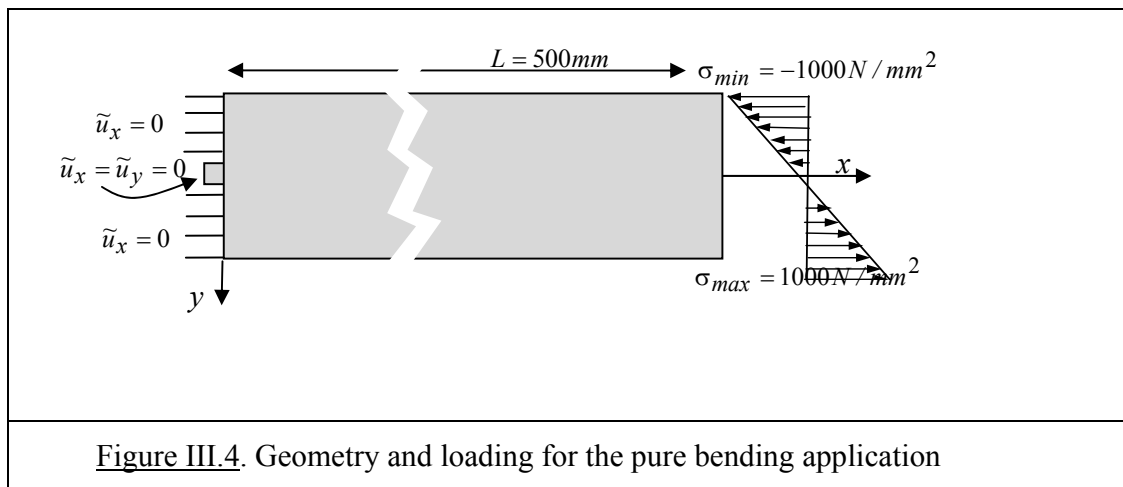
III.7.2. Pure bending

Unit thickness and plane strain conditions are assumed.

The loading and boundary conditions are shown on figure III.4.

The left side is fixed horizontally by symmetry.

In order to prevent the rigid body motion in the vertical direction, a small appendix is added to the left side and fixed both in the horizontal and the vertical directions.

Figure III.5 illustrates the Voronoi cells.

Figure III.4. Geometry and loading for the pure bending application

Figure III.5. Voronoi cells for the pure bending application (222 nodes, random=3)

This is a classical problem of the Theory of Elasticity, the analytical solution of which is known. The strain energy stored in the deformed beam is given by:

$$W_I = \int_A U_0 \, dA \tag{III.68}$$

With

$$M = \int_A \sigma Y \, dA = \frac{\sigma_{max}}{h} I \quad ; \quad I = \int_A y^2 \, dA = \frac{2h^3}{3} \quad ; \quad \sigma_{xx} = \frac{M}{I} Y , \tag{III.69}$$

the theoretical value of the stored energy becomes:

$$W_I\_theory = \frac{1}{2} \int_A \sigma_{ij}\varepsilon_{ij}dA = \frac{1}{2}\frac{M^2L(1-v^2)}{EI} \qquad \text{(III.70)}$$

On the other hand, from the numerical calculation, we get

$$W_I\_num = \sum_{K=1}^{N} \frac{1}{2}\left\{\sigma^K\right\}^T\left\{\varepsilon^K\right\}A_K \qquad \text{(III.71)}$$

With $E = 10^8 MPa$, $v = 0.3$ and the values of σ_{max}, h, L (figure III.4), we get:

$W_I\_theory = 75.8J$

In order to study the influence of the number of nodes and of their distribution, the following procedure has been developed:

a. create a regular pattern of nodes with (n_X+1) nodes in direction X and (n_Y+1) nodes in direction Y;
    the spacings of the nodes in directions X and Y are respectively:
    $\Delta_X = L/n_X$; $\Delta_Y = 2h/n_Y$

b. move the interior nodes randomly about their previous position by the quantities:
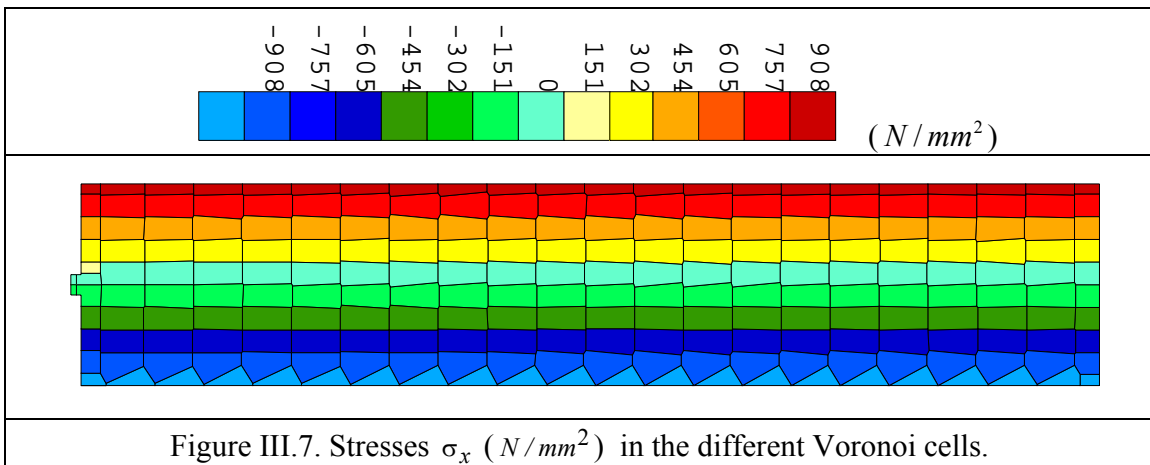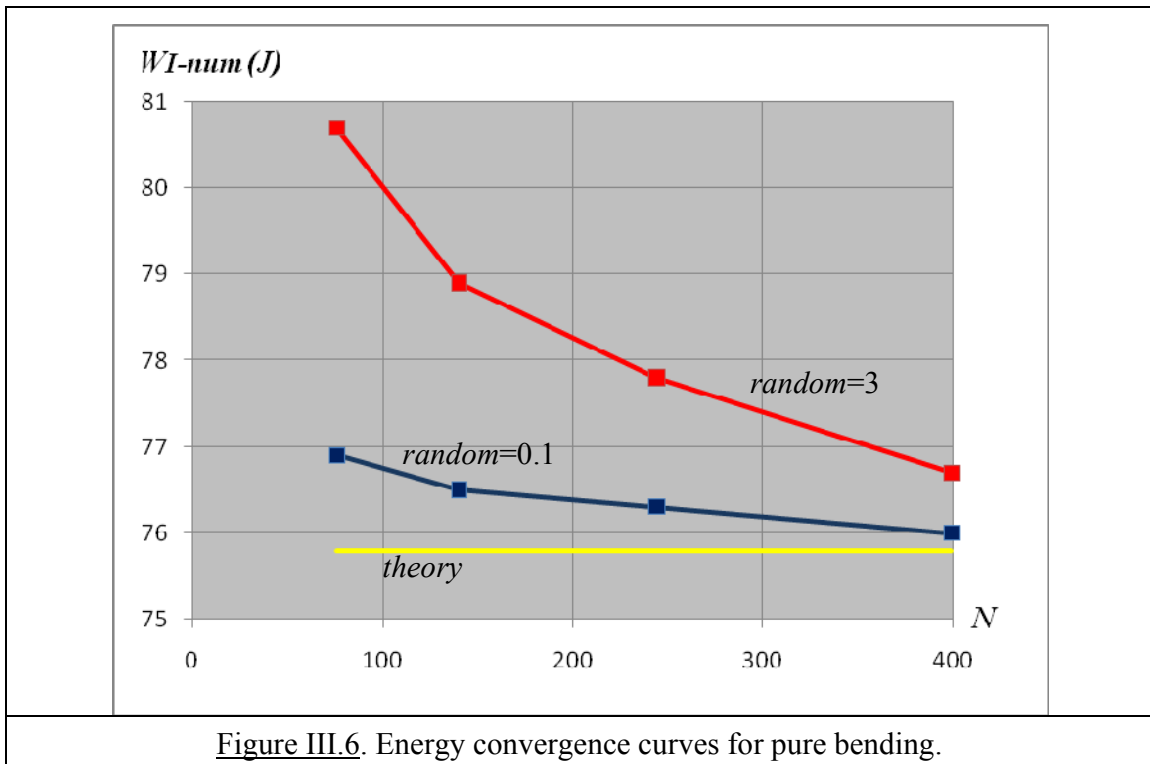
    $$d_X = \frac{random}{5}d_r\Delta_X \;\; ; \;\; d_Y = \frac{random}{5}d_r\Delta_Y \text{ where } -0.5 \le d_r \le +0.5 \text{ is a uniformly}$$

    distributed random number and $0 \le random \le 5$ is a user defined value.

Nodes moving outside the domain are removed.

The results of different calculations are given in table III.7 and summarized in figure III.6 which shows that, with the same *random* value, the results of cases with a more regular Voronoi cell pattern are closer to the theoretical value.

For the case *random* = 0.1, $nx = 20$, $ny = 8$, figure III.7 shows the stresses σ_x in the different Voronoi cells.

Table III.7. Energy results for the pure bending test			
random = 0.1			
n_X	n_Y	N (nb. of nodes)	W_I_num (J)
10	4	76	76.9
15	6	140	76.5
20	8	244	76.3
20	16	399	76.0
random = 3			
n_X	n_Y	N (nb. of nodes)	W_I_num (J)
10	4	78	80.7
15	6	140	78.9
20	8	222	77.8
20	16	398	76.7

Figure III.6. Energy convergence curves for pure bending.

Figure III.7. Stresses σ_x (N/mm^2) in the different Voronoi cells.

To study the effect of near incompressibility, the calculations have also been performed for $\nu = 0.49, 0.499$ and 0.4999.

In addition to the convergence on the energy, the convergence on the displacements has also been considered.

To this end, the following norm has been used:

$$L2norm = \frac{\sum\limits_{i=1}^{N} \sqrt{(u_i^{analy} - u_i^{num}) * (u_i^{analy} - u_i^{num})}}{f_{max} * N} \tag{III.72}$$

where u_i^{analy} are the nodal displacements computed from the analytical solution while u_i^{num} are the nodal displacements obtained by the present numerical method.

$f_{max} = \dfrac{M(1 - v^2)}{2EI} L^2 = \dfrac{\sigma_{max}(1 - v^2)}{2Eh} L^2$ is the maximum theoretical displacement of the beam axis.

N is the number of nodes.

Figures III.8 and III.9 show the convergence curves of the displacements and of the energy for the different values of Poisson's ratio.

Although there is no formal proof, the results obtained in this section and in the preceding one tend to show that incompressibility locking is avoided in the present formulation.
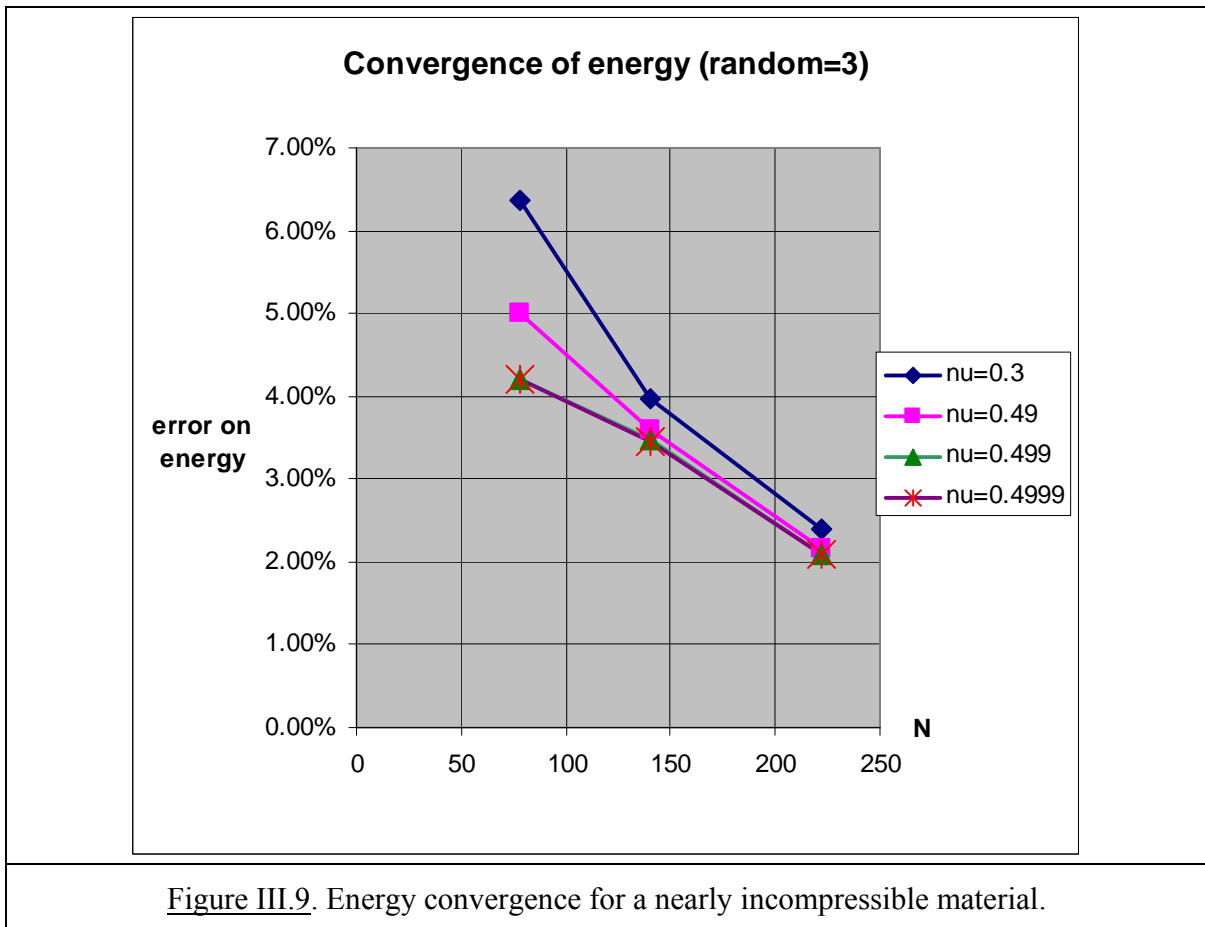

Figure III.8. Displacements convergence for a nearly incompressible material.
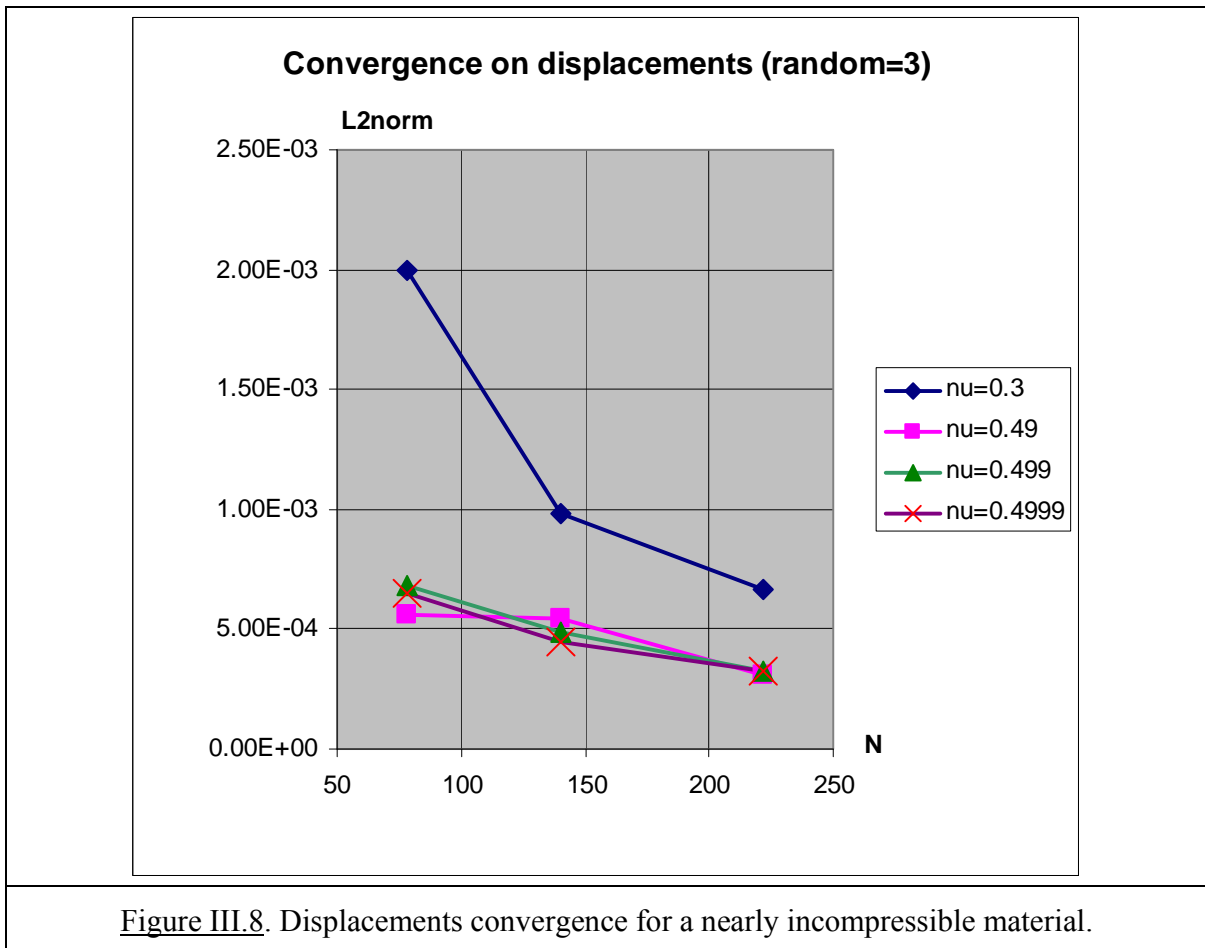
Figure III.9. Energy convergence for a nearly incompressible material.

III.7.3. Square membrane with a circular hole

The material parameters are: $E = 200000 N / mm^2$ and $\nu = 0.3$

The geometry and the loading conditions are defined in figure III.10.

Unit thickness and plane strain conditions are assumed.

The strain energy convergence has been studied for different numbers of integration points on the edges of the Voronoi cells (NP) and different numbers of nodes (N).

It has been compared with the results of the finite elements method (FEM).

For the finite element analyses, classical 4 nodes isoparammetric elements have been used with 4 Gauss integration points for the numerical integrations on the area of the elements. The numbers of nodes used (N_{el}) are approximately the same as for the calculations performed with the present approach.

Table III.8 gives the results.

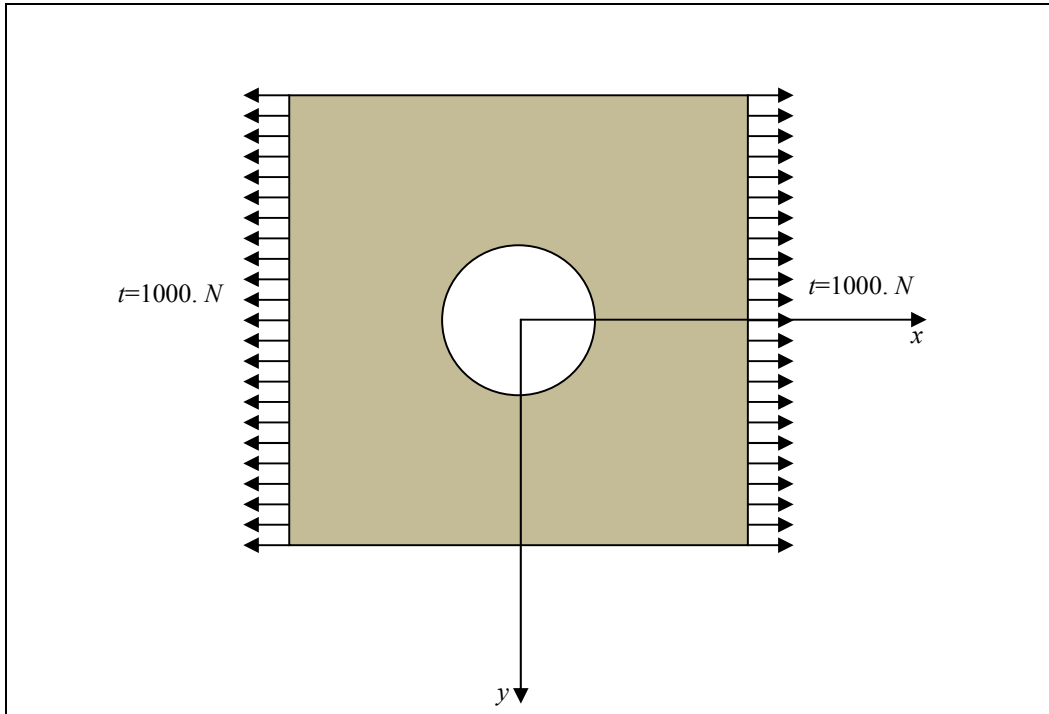The corresponding curves are drawn on figure III.11.

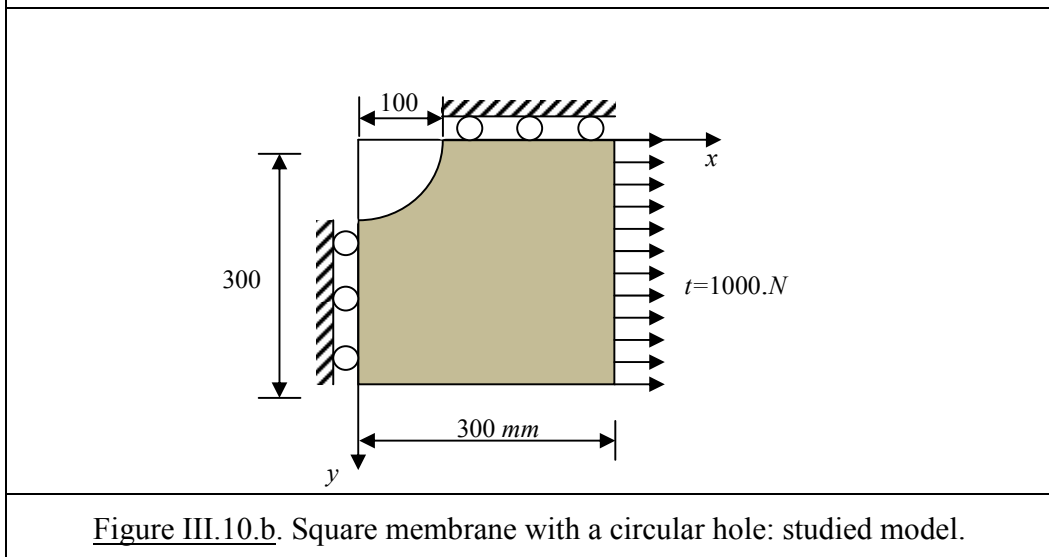Figure III.10.a. Square membrane with a circular hole: geometry and loading.

Figure III.10.b. Square membrane with a circular hole: studied model.

Table III.8. Strain energy (*J*) for the square membrane with a circular hole					
Present method				Finite elements	
N	*NP=1*	*NP=2*	*NP=10*	*N_{el}*	*NP=4*
36	290614	285524	286084	33	238823
121	284496	282707	282874	119	276975
441	281741	281070	281146	445	279986
1681	280715	280517	280542	1645	280100

Figure III.11. Square membrane with a circular hole.
Strain energy convergence.
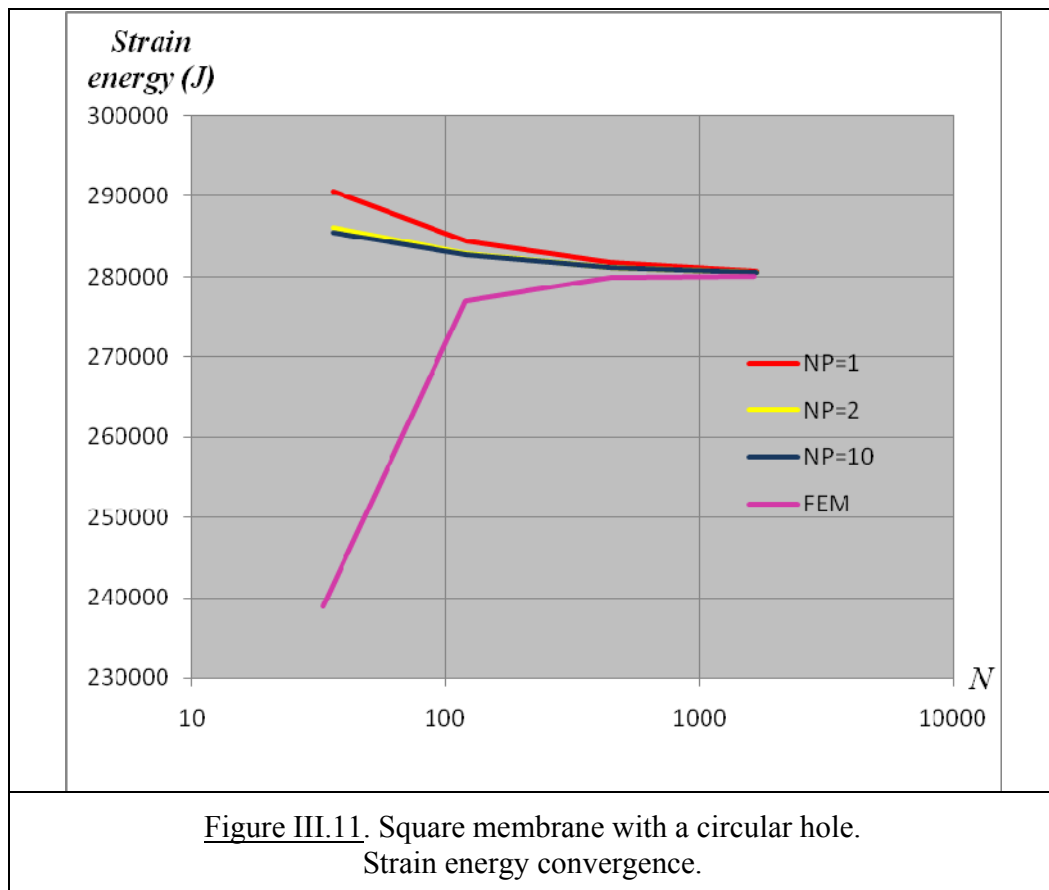
It is clearly seen that the present approach converges from above while the finite element method converges from below in the present case. It is also made clear that, for the same number of nodes, the present approach is closer to the converged value.

The convergence of the stress concentration coefficient is also studied. It is defined as:

$$k = \frac{\sigma_{x.max}}{\sigma_{net}} \quad \text{where} \quad \sigma_{net} = \frac{total\ force\ in\ direction\ x}{net\ cross\ section} = \frac{300 \cdot 1000}{300 - 100} = 1500\ N/mm^2$$

The values are given in tables III.9 and III.10. Figure II.12 illustrates the convergence of *k*.

Table III.9. Square membrane with a circular hole Maximum stress near the hole $\sigma_{x,max}$ (N/mm^2)			
N	*NP=1*	*NP=2*	*NP=10*
36	3663.72	3577.28	3559.7
121	3815.36	3749.17	3751.61
441	3910.19	3891.34	3890.16
1681	3993.57	3995.68	3993.17

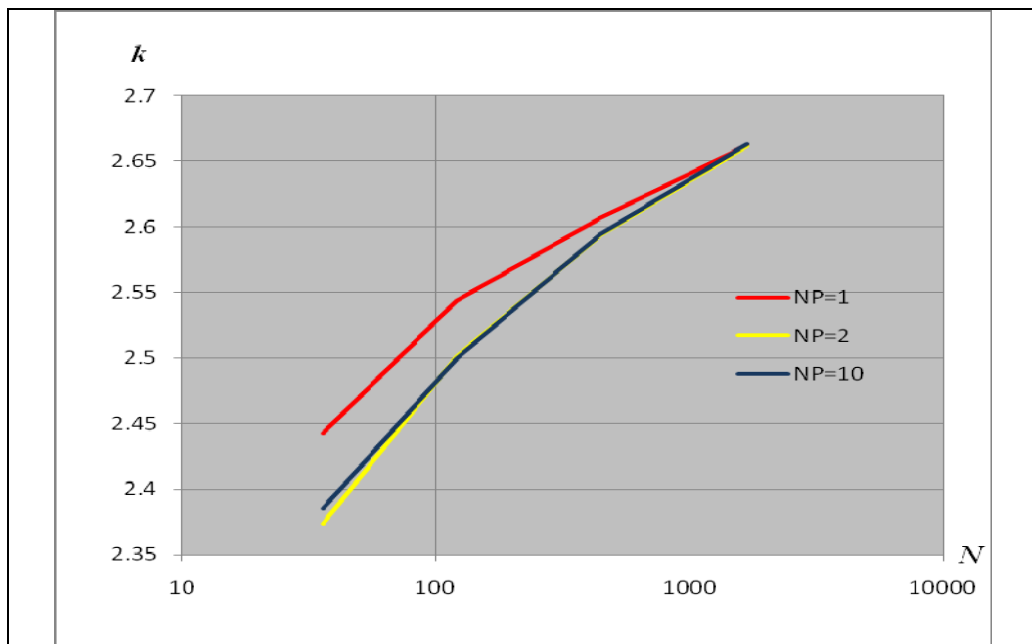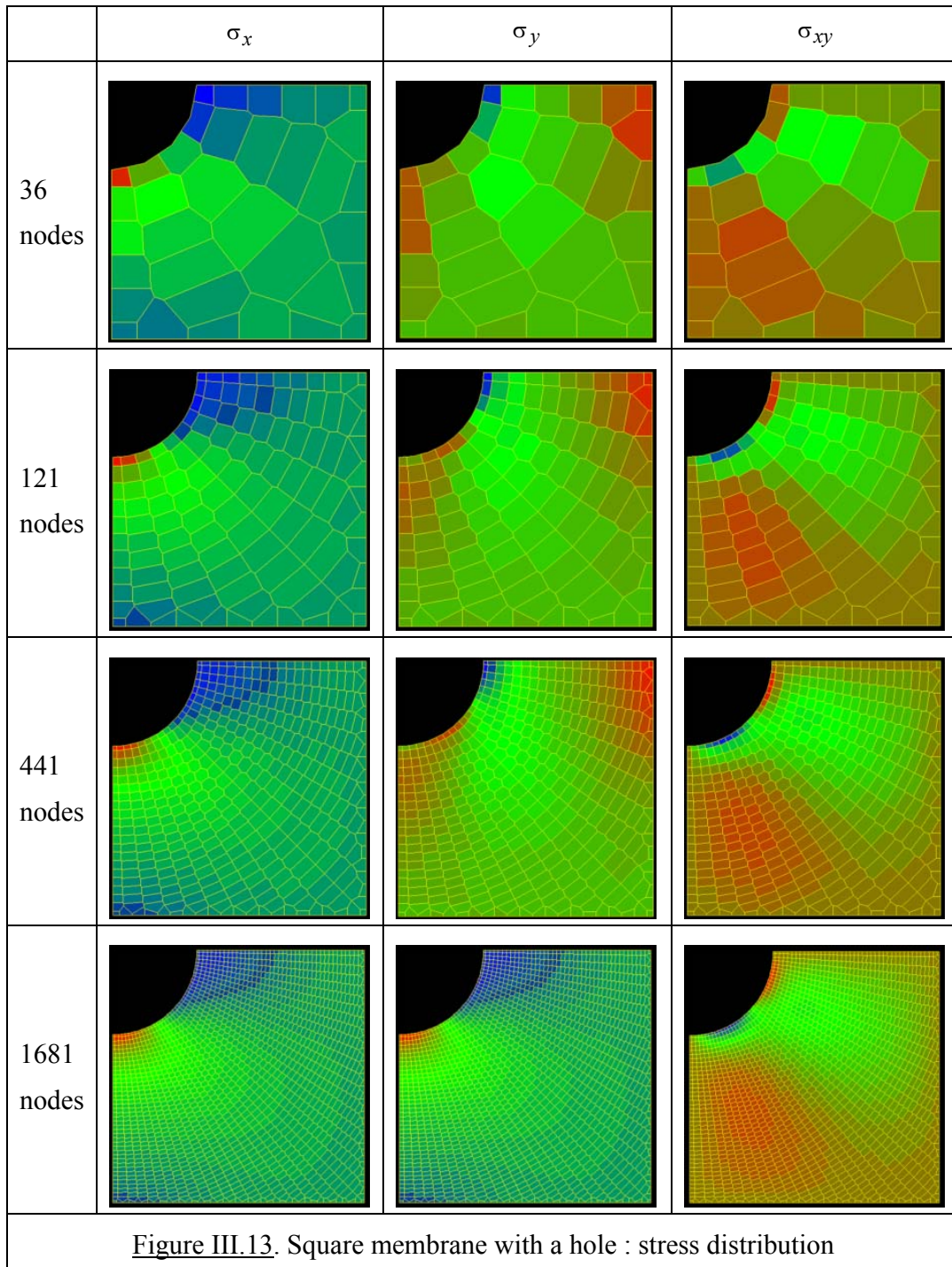| Table III.10. Square membrane with a circular hole Stress concentration coefficient			
N	*NP=1*	*NP=2*	*NP=10*
36	2.4425	2.3849	2.3731
121	2.5436	2.4994	2.5011
441	2.6068	2.5942	2.5934
1681	2.6624	2.6638	2.6621

Figure III.12. Square membrane with a circular hole.

Stress concentration coefficient.

Finally, figure III.13 illustrates the evolution of the stress distribution with the number of nodes.

	σ_x	σ_y	σ_{xy}
36 nodes			
121 nodes			
441 nodes			
1681 nodes			
Figure III.13. Square membrane with a hole : stress distribution			

Figure III.13. Square membrane with a hole : stress distribution

III.8. Conclusion

The Fraeijs de Veubeke variational principle has been used to develop a natural neighbours method in which the displacements, stresses, strains and surface support reactions can be discretized separately.

It has been shown that the additional degrees of freedom linked with the assumed stresses and strains can be eliminated at the level of the Voronoi cells, finally leading to a system of equations of the same size as in the classical displacement-based method.

With the present approach, in the absence of body forces, the calculation of integrals over the area of the domain is avoided: only integrations on the edges of the Voronoi cells are required, for which classical Gauss numerical integration with 2 integration points is sufficient to pass the patch test. In addition, the derivatives of the nodal shape functions are not required in the resulting formulation.

Hence, the properties of the "stabilized nodal integration method" are recovered using a different approach.

These two methods present a clear advantage over more classical methods using integrations over the area of the domain with the help of a sometimes very high number of integration points.

Concerning the boundary conditions, displacements can be imposed in 2 ways.

- In the spirit of the FdV variational principle, boundary conditions of the type $u_i = \tilde{u}_i$ on S_u can be imposed in the average sense; hence, any function $\tilde{u}_i = \tilde{u}_i(s)$ can be accommodated by the method;

- However, since the natural neighbours method is used, the interpolation of displacements on the solid boundary is linear between 2 adjacent nodes. So, if the imposed displacements $\tilde{u}_i$ are linear between 2 adjacent nodes, they can be imposed exactly. This is obviously the case with $\tilde{u}_i = 0$. In such a case, it is equivalent to impose the displacements of these 2 adjacent nodes to zero.

On the other hand, the patch tests and the calculations on the bending case tend to show that the present method allows solving problems involving nearly incompressible materials without locking.